

Phenomenological aspects of a TeV-scale alternative left-right model

 M. Ashry^{1,2,*} and S. Khalil^{2,3,†}
¹*Department of Mathematics, Faculty of Science, Cairo University, 12613 Giza, Egypt*
²*Center for Fundamental Physics, Zewail City of Science and Technology, Sheikh Zayed, 12588 Giza, Egypt*
³*Department of Mathematics, Faculty of Science, Ain Shams University, 11566 Cairo, Egypt*

(Received 3 November 2014; published 8 January 2015; corrected 28 August 2017)

We revisit the alternative left-right symmetric model, motivated by the superstring-inspired E_6 model. We systematically analyze the constraints imposed by theoretical and experimental bounds on the parameter space of this class of models. We perform a comprehensive analysis of the Higgs sector and show that three neutral CP -even and two CP -odd Higgs bosons in addition to two charged Higgs bosons can be light, of $\mathcal{O}(100)$ GeV. We emphasize that the predictions of this model for the signal strengths of Higgs decays are consistent with the standard model expectations. We also explore discovery signatures of the exotic down-type quark, which is one of the salient predictions of this model.

DOI: 10.1103/PhysRevD.91.015009

PACS numbers: 12.10.Dm, 14.65.Jk

I. INTRODUCTION

The discovery of neutrino masses and oscillations confirmed the fact that, although the standard model (SM) is extremely accurate, it is still incomplete. The left-right model (LRM) is the most natural extension of the SM that accounts for the measured neutrino masses and provides an elegant understanding for the origin of the parity violation in low-energy weak interactions [1–8]. The LRM is based on the gauge group $SU(3)_C \times SU(2)_L \times SU(2)_R \times U(1)_{(B-L)/2} \times P$, where P is the discrete parity symmetry. In the LRM, standard model fermions are assigned in the following left- or right-handed doublets:

$$\begin{aligned} Q_L &\equiv \begin{pmatrix} u_L \\ d_L \end{pmatrix}, & \psi_L &\equiv \begin{pmatrix} \nu_L \\ e_L \end{pmatrix} \\ \& \quad Q_R &\equiv \begin{pmatrix} u_R \\ d_R \end{pmatrix}, & \psi_R &\equiv \begin{pmatrix} \nu_R \\ e_R \end{pmatrix}. \end{aligned} \quad (1)$$

The parity symmetry $Q_L, \psi_L \leftrightarrow Q_R, \psi_R$ implies that the gauge couplings of left- and right-handed $SU(2)$ are equal, i.e., $g_L = g_R \equiv g$.

The Higgs sector of the LRM consists of (i) bidoublet $\Phi(1, 2, 2^*, 0)$, which is required to construct the SM Yukawa couplings of quarks and leptons, and (ii) two scalar triplets $\Delta_L(1, 3, 0, 2)$ and $\Delta_R(1, 0, 3, 2)$ that break $U(1)_{(B-L)/2}$ and generate neutrino Majorana masses. At the high-energy scale, well above the electroweak breaking scale, the $SU(2)_R \times U(1)_{(B-L)/2} \times P$ symmetry is broken down to $U(1)_Y$ by the vacuum expectation value (vev) of the neutral component of Δ_R , and hence the right-handed Majorana neutrino mass is generated. In this type of

models, the hypercharge Y is defined as $Y = T_{3R} + (B - L)/2$, where T_{3R} is the third component of the right-handed isospin. At lower energy scales, Φ and Δ_L acquire vevs that break $SU(2)_L \times U(1)_Y$ down to $U(1)_{em}$. It is worth mentioning that in the conventional LRM one gets the following estimate for the associated vevs: $\langle \Delta_L \rangle = v_L \lesssim \mathcal{O}(1)$ GeV, $\langle \Delta_R \rangle = v_R \gtrsim \mathcal{O}(10^{11})$ GeV, and $\langle \Phi \rangle = \text{diag}\{\kappa, \kappa'\}$ with $\kappa' \ll \kappa$ and $\kappa \sim \mathcal{O}(100)$ GeV [1,3,4].

It turns out that the Higgs sector of the LRM, in particular the Higgs triplets, may induce tree-level flavor-violating processes that contradict the current experimental limits. Therefore, it is usually assumed that $SU(2)_R \times U(1)_{(B-L)/2}$ is broken at a very high-energy scale. In this case, it is not possible to detect any residual effect for $SU(2)_R$ gauge symmetry at the TeV scale in the LHC. This motivated Ernest Ma, in his pioneering work in 1987 [9], to study variants of the conventional LRM. He has shown that the superstring-inspired E_6 model may lead to two types of left-right models. The first one is the canonical LRM, while the second one is what is known as the alternative left-right model (ALRM) [10,11], where the fermion assignments are different from those in the conventional LRM in the following: (i) an extra quark, d'_R , instead of d_R , is combined with u_R and forms $SU(2)_R$ doublet, and (ii) an extra lepton, n_R , instead of ν_R , is combined with e_R and forms $SU(2)_R$ doublet. Therefore, the right-handed neutrino ν_R is a true singlet and is no longer a part of the right-handed doublet.

It is remarkable that E_6 is a complex Lie group of rank 6. It includes the $SO(10)$ group, so it is a good candidate for grand unification. Some string theories (Heterotic string) predict that the low-energy effective model is symmetric under E_6 . Depending on the string model, E_6 may be broken to $SO(10)$ and then to the conventional left-right model, or it may have another branch of symmetry breaking that leads to the alternative left-right model that we consider. The particle content of the ALRM, derived from E_6 model, contains

*mustafa@sci.cu.edu.eg

†skhalil@zewailcity.edu.eg

more particles than those in the conventional LRM obtained from $SO(10)$. This can be simply understood from the fact that the fundamental representation 27 of E_6 is equivalent to the fundamental representation 16 of $SO(10)$ plus its 10 and singlet representations. In the conventional LRM, all non-SM particles are decoupled and can be quite heavy. However, in the ALRM, they are involved with the SM fermions and will have low-energy consequences. Furthermore, another important difference between the ALRM and the conventional LRM is the fact that tree-level flavor-changing neutral currents are naturally absent so that the $SU(2)_R$ breaking scale can be of order TeV, allowing to several interesting signatures at the LHC. As the ALRM is a low-energy effective model of the supersymmetric E_6 model, the gauge couplings are not unified within the ALRM. They are unified in the underlying E_6 model, similar to the unification of SM gauge couplings in supersymmetric $SU(5)$.

In this paper, we aim at providing a comprehensive analysis for the phenomenological implications of the ALRM, with emphasis on the possible signatures of this model at the LHC. There are couple of recent papers [11,12] that discuss specific phenomenological aspects of the ALRM, namely, the dark matter search and Z' and W' signals at the LHC. Our goal here is twofold. The first is to analyze the Higgs sector of the ALRM and check if the recent results reported by ATLAS and CMS experiments on Higgs production and decays can be accommodated. The second is to explore the discovery signature of the exotic down-type quarks associated with this type of models at the LHC.

The latest results of ATLAS and CMS collaborations [13,14] confirmed the Higgs discovery with mass around 125 GeV, through Higgs decay channels: $H \rightarrow \gamma\gamma$, $H \rightarrow ZZ^{(*)} \rightarrow 4l$, and $H \rightarrow WW^{(*)} \rightarrow l\nu l\nu$ at integrated luminosities of 5.1 fb^{-1} taken at energy $\sqrt{s} = 7 \text{ TeV}$ and 19.6 fb^{-1} taken at $\sqrt{s} = 8 \text{ TeV}$. These results still indicate possible discrepancies between their results for signal strengths in these channels [15–18]. We show that our ALRM has a rich Higgs sector and consists of one bidoublet and two left-handed and right-handed doublets. Therefore, one obtains four neutral CP -even and two CP -odd Higgs bosons, in addition to two charged Higgs bosons. It turns out that most of these Higgs bosons can be light, of the order of the electroweak scale, and can be accessible at the LHC. We also find that the contributions of the charged Higgs bosons to the decay rate of $H \rightarrow \gamma\gamma$ are not significant. Furthermore, we show that, due to the mixing among the neutral CP -even Higgs bosons, the couplings of the SM-like Higgs, which is the lightest one, with the top quark and W -gauge boson are slightly modified respect to the SM ones. Therefore, the ALRM predictions for signal strengths of Higgs decays, in particular, $H \rightarrow \gamma\gamma$ and $H \rightarrow W^+W^-$, are consistent with the SM expectation.

Another salient feature of the ALRM is the presence of an extra down-type quark, d' . We analyze the striking

signature of this exotic quark at the LHC. We show that the most promising d' -production channel is $gg \rightarrow \bar{d}'d'$, due to the direct coupling of d' to gluons with a strong coupling constant and color factor. Then, d' decays to a jet and lepton plus missing energy. We find that the cross section of this process is of $\mathcal{O}(1)$ fb, which can be probed at the LHC with 14 TeV center-of-mass energy.

The paper is organized as follows. In Sec. 2, we briefly review the TeV scale ALRM. Section 3 is devoted to the Higgs sector, in particular, for studying the mixing matrix of the Higgs bosons and investigating the existence of two light charged Higgs bosons. In Sec. 4, we focus on the Higgs decay into a diphoton in the ALRM. The discovery signatures of extra quark d' at the LHC is discussed in Sec. 5. Finally, we give our conclusions in Sec. 6.

II. ALTERNATIVE LEFT-RIGHT SYMMETRIC MODEL

We consider an ALRM based on $SU(3)_C \times SU(2)_L \times SU(2)_R \times U(1)_{(B-L)/2} \times S$, where S is a discrete symmetry imposed to distinguish between scalars and their dual scalars. The fermion content of this model, with its charge assignments, is presented in Table I [19]. As can be seen from this table, extra quarks and leptons are predicted as in all E_6 -based left-right models.

The Higgs sector of our ALRM consists of an $SU(2)_R$ scalar doublet χ_R to break $SU(2)_R \times U(1)_{(B-L)/2}$ in addition to $SU(2)_L$ scalar doublet χ_L and scalar bidoublet Φ that

TABLE I. Particle content and its quantum numbers in the ALRM.

Fields	$SU(3)_C \times SU(2)_L \times SU(2)_R \times U(1)_{(B-L)/2}$	S
Fermions		
$Q_L \equiv \begin{pmatrix} u \\ d \end{pmatrix}_L$	$(3, 2, 1, +\frac{1}{6})$	0
$Q_R \equiv \begin{pmatrix} u \\ d' \end{pmatrix}_R$	$(3, 1, 2, +\frac{1}{6})$	$-\frac{1}{2}$
d'_L	$(3, 1, 1, -\frac{1}{3})$	-1
d_R	$(3, 1, 1, -\frac{1}{3})$	0
$\psi_L \equiv \begin{pmatrix} \nu \\ e \end{pmatrix}_L$	$(1, 2, 1, -\frac{1}{2})$	0
$\psi_R \equiv \begin{pmatrix} n \\ e \end{pmatrix}_R$	$(1, 1, 2, -\frac{1}{2})$	$+\frac{1}{2}$
n_L	$(1, 1, 1, 0)$	+1
ν_R	$(1, 1, 1, 0)$	0
Higgs		
$\Phi \equiv \begin{pmatrix} \phi_1^0 & \phi_1^+ \\ \phi_2^- & \phi_2^0 \end{pmatrix}$	$(1, 2, 2^*, 0)$	$-\frac{1}{2}$
$\chi_L \equiv \begin{pmatrix} \chi_L^+ \\ \chi_L^0 \end{pmatrix}$	$(1, 2, 1, +\frac{1}{2})$	0
$\chi_R \equiv \begin{pmatrix} \chi_R^+ \\ \chi_R^0 \end{pmatrix}$	$(1, 1, 2, +\frac{1}{2})$	$+\frac{1}{2}$

break $SU(2)_L \times U(1)_Y$. The detailed quantum numbers of these Higgs bosons are presented in Table I [19].

In this case, the most general left-right symmetric Yukawa Lagrangian is given by

$$\mathcal{L}_Y = \bar{Q}_L Y^q \tilde{\Phi} Q_R + \bar{Q}_L Y_L^q \chi_L d_R + \bar{Q}_R Y_R^q \chi_R d'_L + \bar{\psi}_L Y^\ell \Phi \psi_R + \bar{\psi}_L Y_L^\ell \tilde{\chi}_L \nu_R + \bar{\psi}_R Y_R^\ell \tilde{\chi}_R n_L + \bar{\nu}_R^c M_R \nu_R + \text{H.c.}, \quad (2)$$

where $\tilde{\Phi}$ is the dual of the scalar bidoublet Φ , defined as $\tilde{\Phi} = \tau_2 \Phi^* \tau_2$, and $\tilde{\chi}_{L,R}$ are the dual of the scalar doublets $\chi_{L,R}$, defined as $\tilde{\chi}_{L,R} = i\tau_2 \chi_{L,R}^*$. Note that the Yukawa terms like $\bar{\psi}_L \tilde{\Phi} \psi_R$ and $\bar{Q}_L \tilde{\Phi} Q_R$ are forbidden by the discrete S symmetry only. A detailed discussion on the Higgs potential and the associated vevs will be given in the next section. Here, we assume a nonvanishing vev of χ_R , $\langle \chi_R \rangle = v_R/\sqrt{2}$ of order TeV with vevs of χ_L and Φ , given by $\langle \chi_L \rangle = v_L/\sqrt{2}$ and $\langle \Phi \rangle = \text{diag}\{0, k/\sqrt{2}\}$. The breaking of $SU(2)_R \times U(1)_{(B-L)/2}$ down to $U(1)_Y$ leaves the discrete symmetry $L = S + T_{3R}$ unbroken, if the vev of ϕ_1^0 (which has $L = -1$) is zero, while ϕ_2^0 (with $L = 0$) could have a nonvanishing vev. In this case, one can easily show that the quarks u , d , and d' and the charged leptons ℓ , in addition to the singlet fermion n , which is called a scotino, acquire the masses

$$m_u = \frac{1}{\sqrt{2}} Y^q v \sin \beta, \quad m_d = \frac{1}{\sqrt{2}} Y_L^q v \cos \beta, \quad m_{d'} = \frac{1}{\sqrt{2}} Y_R^q v_R, \quad (3)$$

$$m_\ell = \frac{1}{\sqrt{2}} Y^\ell v \sin \beta, \quad m_n = \frac{1}{\sqrt{2}} Y_R^\ell v_R, \quad (4)$$

where $\tan \beta = k/v_L$ and $\sqrt{v_L^2 + k^2} = v \equiv 246$ GeV. Moreover, the neutrino mass matrix is given by

$$M_\nu = \left(\begin{array}{c|cc} & \nu_L^c & \nu_R \\ \hline \bar{\nu}_L & 0 & m_{\nu D} \\ \bar{\nu}_R^c & m_{\nu D}^T & M_R \end{array} \right), \quad (5)$$

where $m_{\nu D} = Y_L^\ell v_L/\sqrt{2}$. The mass M_R is not related to the $SU(2)_R$ symmetry-breaking scale, so it can be quite large. This matrix can be diagonalized by a unitary matrix, $V_\nu M_\nu V_\nu^T \approx \text{diag}(m_{\nu_l}, m_{\nu_h})$, where m_{ν_l} and m_{ν_h} are the well-known seesaw mass eigenvalues of the light and heavy neutrinos, respectively:

$$m_{\nu_l} \approx m_{\nu D} M_R^{-1} m_{\nu D}^T, \quad m_{\nu_h} \approx M_R. \quad (6)$$

Now, we turn to the gauge sector of the ALRM; the covariant derivatives of the Higgs bosons are given by

$$D_\mu \Phi = \partial_\mu \Phi - i \frac{g}{2} (\tau^a W_{L_\mu}^a \Phi - \Phi \tau^a W_{R_\mu}^a), \quad (7)$$

$$D_\mu \chi_{L,R} = \partial_\mu \chi_{L,R} - i \frac{g}{2} \tau^a W_{L,R_\mu}^a \chi_{L,R} - i \frac{g_{BL}}{2} B_\mu \chi_{L,R}, \quad (8)$$

where g_{BL} is the gauge coupling of the $U(1)_{(B-L)/2}$ group. After the spontaneous breaking of left-right symmetry down to electroweak and then down to electromagnetism, the associated gauge bosons acquire masses, through the nonvanishing vevs of χ_R , Φ , and χ_L . Because of the vanishing vev of $\phi_1^0 \in \Phi$, the mixing between W_L^\pm and W_R^\mp is identically zero. Thus, the physical eigenstates are given by SM gauge bosons $W^\pm = W_L^\pm$ and $W'^\pm = W_R^\pm$ with masses

$$M_W^2 = \frac{1}{4} g^2 (k^2 + v_L^2) = \frac{1}{4} g^2 v^2, \quad (9)$$

$$M_{W'}^2 = \frac{1}{4} g^2 (k^2 + v_R^2). \quad (10)$$

The experimental searches for W' at the LHC through their decays to electron/muon and neutrino lead to $M_{W'} \gtrsim 2.5$ TeV [20,21]. The interactions of our W' with the SM fermions are given by

$$\mathcal{L}_{\text{gauge}}^{W'} = -\frac{ig}{\sqrt{2}} \bar{u} \gamma^\mu W_\mu'^+ V_{\text{CKM}}^u P_R d' - \frac{ig}{\sqrt{2}} \bar{d}' \gamma^\mu W_\mu'^- V_{\text{CKM}}^{d'} P_R u - \frac{ig}{\sqrt{2}} \bar{n} \gamma^\mu W_\mu'^+ U_{\text{MNS}}^n P_R e - \frac{ig}{\sqrt{2}} \bar{e} \gamma^\mu W_\mu'^- U_{\text{MNS}}^{e'} P_R n. \quad (11)$$

Thus, W' can decay into an electron and singlet fermion (scotino) n , which appears at the LHC as missing energy. Therefore, the above-mentioned lower bound on $M_{W'}$ is applicable in our ALRM. This implies that $v_R \gtrsim \mathcal{O}(1)$ TeV. The situation of the neutral gauge bosons W_L^3 , W_R^3 , and B is more involved. One can show that their mass matrix is given by

$$\left(\begin{array}{c|ccc} & W_L^3 & W_R^3 & B \\ \hline W_L^3 & \frac{1}{4} g^2 (k^2 + v_L^2) & -\frac{1}{4} g^2 k^2 & -\frac{1}{4} g g_{BL} v_L^2 \\ W_R^3 & -\frac{1}{4} g^2 k^2 & \frac{1}{4} g^2 (k^2 + v_R^2) & -\frac{1}{4} g g_{BL} v_R^2 \\ B & -\frac{1}{4} g g_{BL} v_L^2 & -\frac{1}{4} g g_{BL} v_R^2 & \frac{1}{4} g_{BL}^2 (v_L^2 + v_R^2) \end{array} \right). \quad (12)$$

One can define $s_w \equiv \sin \theta_w = e/g$, and with $c_w \equiv \cos \theta_w$, then $g_{BL} = e/\sqrt{c_w^2 - s_w^2}$. It is more convenient to work in the basis (A, Z_L, Z_R) , where

$$\begin{pmatrix} A \\ Z_L \\ Z_R \end{pmatrix} = \begin{pmatrix} s_w & s_w & \sqrt{c_w^2 - s_w^2} \\ c_w & -s_w^2/c_w & -s_w \sqrt{c_w^2 - s_w^2}/c_w \\ 0 & \sqrt{c_w^2 - s_w^2}/c_w & -s_w/c_w \end{pmatrix} \begin{pmatrix} W_L^3 \\ W_R^3 \\ B \end{pmatrix}. \quad (13)$$

In this case, one can show that the mass eigenvalue of the gauge boson A is identically zero. Therefore, this gauge boson is the photon that should remain massless after symmetry breaking. The exact eigenstates Z, Z' are obtained as

$$\begin{pmatrix} Z \\ Z' \end{pmatrix} = \begin{pmatrix} \cos \vartheta & \sin \vartheta \\ -\sin \vartheta & \cos \vartheta \end{pmatrix} \begin{pmatrix} Z_L \\ Z_R \end{pmatrix}. \quad (14)$$

The mixing angle ϑ is defined as

$$\tan 2\vartheta = \frac{2M_{LR}^2}{M_{LL}^2 - M_{RR}^2}, \quad (15)$$

where

$$M_{LL}^2 = \frac{g^2 v^2}{4 \cos^2 \theta_w}, \quad (16)$$

$$M_{LR}^2 = \frac{g^2 (v^2 \sin^2 \theta_w - k^2 \cos^2 \theta_w)}{4 \cos^2 \theta_w \sqrt{\cos 2\theta_w}}, \quad (17)$$

$$M_{RR}^2 = \frac{g^2 (2v^2 \sin^4 \theta_w + 2(k^2 + v_R^2) \cos^4 \theta_w - k^2 \sin^2 2\theta_w)}{8 \cos^2 \theta_w \cos 2\theta_w}. \quad (18)$$

The eigenvalues M_Z^2 and $M_{Z'}^2$ are given by

$$M_{Z,Z'}^2 = \frac{1}{2} (M_{LL}^2 + M_{RR}^2 \mp (M_{RR}^2 - M_{LL}^2) \sqrt{1 + \tan^2 2\vartheta}). \quad (19)$$

It is clear that if $v_R \gg v$, i.e., $\vartheta \rightarrow 0$, then $Z \simeq Z_L$ and $Z' \simeq Z_R$. The LHC search for the Z' gauge boson is rather model dependent. However, one may consider $M_{Z'} \gtrsim 2$ TeV as a conservative lower bound [22,23]. In addition, the mixing between Z and Z' should be less than $\mathcal{O}(10^{-3})$.

III. HIGGS SECTOR IN THE ALRM

A. Symmetry breaking

The Higgs sector of our ALRM consists of bidoublet Φ with left and right doublets χ_L and χ_R . The charge assignments of these Higgs bosons are shown in Table I. As mentioned in the previous section, the gauge symmetries $SU(2)_R \times U(1)_{(B-L)/2}$ are spontaneously broken to $U(1)_Y$ through the vev of χ_R , and then $SU(2)_L \times U(1)_Y$ symmetries are broken by vevs of Φ and χ_L . The most general Higgs potential that is invariant under these symmetries is given by [7]

$$\begin{aligned} V(\Phi, \chi_{L,R}) = & -\mu_1^2 \text{Tr}[\Phi^\dagger \Phi] + \lambda_1 (\text{Tr}[\Phi^\dagger \Phi])^2 + \lambda_2 \text{Tr}[\Phi^\dagger \tilde{\Phi}] \text{Tr}[\tilde{\Phi}^\dagger \Phi] - \mu_2^2 (\chi_L^\dagger \chi_L + \chi_R^\dagger \chi_R) + \lambda_3 [(\chi_L^\dagger \chi_L)^2 + (\chi_R^\dagger \chi_R)^2] \\ & + 2\lambda_4 (\chi_L^\dagger \chi_L)(\chi_R^\dagger \chi_R) + 2\alpha_1 \text{Tr}(\Phi^\dagger \Phi)(\chi_L^\dagger \chi_L + \chi_R^\dagger \chi_R) + 2\alpha_2 (\chi_L^\dagger \Phi \Phi^\dagger \chi_L + \chi_R^\dagger \Phi^\dagger \Phi \chi_R) \\ & + 2\alpha_3 (\chi_L^\dagger \tilde{\Phi} \tilde{\Phi}^\dagger \chi_L + \chi_R^\dagger \tilde{\Phi}^\dagger \tilde{\Phi} \chi_R) + \mu_3 (\chi_L^\dagger \Phi \chi_R + \chi_R^\dagger \Phi^\dagger \chi_L). \end{aligned} \quad (20)$$

In the Appendix, we provide a detailed study for the conditions that keep the potential (20) bounded from below. It is remarkable that the copositivity conditions [24,25] for this Higgs potential significantly depend on the signs of the following parameters: $\alpha_{12} = \alpha_1 + \alpha_2$, $\alpha_{13} = \alpha_1 + \alpha_3$, and $\lambda_{12} = \lambda_1 + 2\lambda_2$. Here, we present the case with minimal constraints imposed on the potential parameters:

$$\begin{aligned} \lambda_1 &\geq 0, & \lambda_2 &\leq 0, & \lambda_3 &\geq 0, & \alpha_2 - \alpha_3 &\geq 0, \\ \alpha_{12} &\geq 0, & \alpha_{13} &\geq 0, & \lambda_{12} &\geq 0. \end{aligned} \quad (21)$$

Also for perturbativity, the absolute value of any dimensionless potential parameter is assumed to be less than $\sqrt{4\pi}$. In addition, from the minimization conditions, one finds that the nonvanishing vevs are given by

$$v_L v_R = \frac{-\mu_3 k}{\sqrt{2}(\lambda_4 - \lambda_3)}, \quad (22)$$

$$v_L^2 + v_R^2 = \frac{\mu_2^2 - \alpha_{12} k^2}{\lambda_3}, \quad (23)$$

$$k^2 = \frac{2(\lambda_3 \mu_1^2 - \alpha_{12} \mu_2^2)(\lambda_4 - \lambda_3) + \lambda_3 \mu_3^2}{2(\lambda_1 \lambda_3 - \alpha_{12}^2)(\lambda_4 - \lambda_3)}. \quad (24)$$

We use these equations to determine three parameters (μ_1 , μ_2 , and λ_4) out of the ten free parameters in the Higgs potential (20) in terms of the vevs: $k = v \sin \beta$, $v_L = v \cos \beta$, and $v_R \sim \mathcal{O}(1)$ TeV. Note that since the vevs k , v_L are of the same order and the couplings $\lambda_{3,4} \lesssim \mathcal{O}(1)$, the values of μ_3 can be smaller than v_R .

B. Higgs masses and mixing

We begin by 16 degrees of freedom: 8 of Φ and 8 of χ_L and χ_R . After symmetry breaking, two neutral components of these 16 degrees of freedom will be eaten by the neutral gauge bosons Z and Z' to acquire their masses. In addition, another

four charged components will be eaten by the charged gauge bosons W^\pm and W'^\pm to acquire their masses. Therefore, ten scalars remain as physical Higgs bosons in this class of models. As we will explicitly show, four of them give charged Higgs bosons, two lead to pseudoscalar Higgs bosons, and the remaining four give CP -even neutral Higgs bosons.

(1) Charged Higgs bosons

The mass matrix of the charged Higgs bosons, in the basis $(\phi_1^+ \chi_L^+ \phi_2^+ \chi_R^+)$, is a block diagonal matrix with the following two matrices, which, respectively, correspond to the bases $(\phi_1^+ \chi_L^+)$ and $(\phi_2^+ \chi_R^+)$:

$$M_{1L}^+ = \begin{pmatrix} -(\alpha_2 - \alpha_3)v_L^2 - \frac{\mu_3 v_R}{\sqrt{2}} \cot \beta & (\alpha_2 - \alpha_3)v_L^2 \tan \beta - \frac{\mu_3 v_R}{\sqrt{2}} \\ (\alpha_2 - \alpha_3)v_L^2 \tan \beta - \frac{\mu_3 v_R}{\sqrt{2}} & -(\alpha_2 - \alpha_3)v_L^2 \tan^2 \beta - \frac{\mu_3 v_R}{\sqrt{2}} \tan \beta \end{pmatrix}, \quad (25)$$

$$M_{2R}^+ = \begin{pmatrix} -(\alpha_2 - \alpha_3)v_R^2 - \frac{\mu_3 v_L}{\sqrt{2}} \cot \zeta & (\alpha_2 - \alpha_3)v_R^2 \tan \zeta - \frac{\mu_3 v_L}{\sqrt{2}} \\ (\alpha_2 - \alpha_3)v_R^2 \tan \zeta - \frac{\mu_3 v_L}{\sqrt{2}} & -(\alpha_2 - \alpha_3)v_R^2 \tan^2 \zeta - \frac{\mu_3 v_L}{\sqrt{2}} \tan \zeta \end{pmatrix}, \quad (26)$$

where $\tan \zeta = k/v_R$, in analogy to $\tan \beta$ with left-right switch. These matrices can be diagonalized by the unitary transformations, $V_1^\dagger M_{1L}^+ V_1 = \text{diag}(M_{H_1^\pm}, 0)$ and $V_2^\dagger M_{2R}^+ V_2 = \text{diag}(M_{H_2^\pm}, 0)$, where

$$\begin{pmatrix} \phi_1^+ \\ \chi_L^+ \end{pmatrix} = \underbrace{\begin{pmatrix} \cos \beta & \sin \beta \\ -\sin \beta & \cos \beta \end{pmatrix}}_{V_1} \begin{pmatrix} H_1^+ \\ G_1^+ \end{pmatrix},$$

$$\begin{pmatrix} \phi_2^+ \\ \chi_R^+ \end{pmatrix} = \underbrace{\begin{pmatrix} \cos \zeta & \sin \zeta \\ -\sin \zeta & \cos \zeta \end{pmatrix}}_{V_2} \begin{pmatrix} H_2^+ \\ G_2^+ \end{pmatrix}. \quad (27)$$

The eigenstates G_1^\pm and G_2^\pm are the charged Goldstone bosons eaten by the gauge bosons W^\pm and W'^\pm to acquire their masses. The charged Higgs bosons masses are

$$M_{H_1^\pm}^2 = -(\alpha_2 - \alpha_3)v_L^2 \sec^2 \beta - \sqrt{2}\mu_3 v_R \csc 2\beta, \quad (28)$$

$$M_{H_2^\pm}^2 = -(\alpha_2 - \alpha_3)v_R^2 \sec^2 \zeta - \sqrt{2}\mu_3 v_L \csc 2\zeta. \quad (29)$$

From these expressions, one can show that the mass of the charged Higgs can be of $\mathcal{O}(100)$ GeV.

(2) CP -odd Higgs bosons

We now turn to the neutral Higgs physical fields and their masses. This can be easily obtained if one develops the neutral components of the bidoublets Φ and the doublets $\chi_{L,R}$ around their vacua into real and imaginary parts, i.e.,

$$\phi_i^0 = \frac{1}{\sqrt{2}}(v_i + \phi_i^{0R} + i\phi_i^{0I}), \quad i = 1, 2, L, R, \quad (30)$$

where $v_1 = 0$, $v_2 = k$, and $\phi_{L,R} = \chi_{L,R}$. In this case, the squared mass matrix of neutral Goldstone and CP -odd Higgs bosons is given by

$$M_{ij}^2 = \left. \frac{\partial^2 V(\Phi, \chi_{L,R})}{\partial \phi_i^{0I} \partial \phi_j^{0I}} \right|_{\langle \phi_i^{0R} \rangle = \langle \phi_j^{0I} \rangle = 0}. \quad (31)$$

One finds that this mass matrix in the basis of $(\phi_1^{0I}, \phi_2^{0I}, \chi_L^{0I}, \chi_R^{0I})$ is factored as a product of the squared mass of ϕ_1^{0I} , which is totally decoupled due to the fact that we have $v_1 = 0$, times the following 3×3 squared mass matrix of $(\phi_2^{0I}, \chi_L^{0I}, \chi_R^{0I})$:

$$M_I^2 = -\frac{k\mu_3}{2\sqrt{2}} \begin{pmatrix} \cot \beta \cot \zeta & -\cot \zeta & \cot \beta \\ -\cot \zeta & \tan \beta \cot \zeta & -1 \\ \cot \beta & -1 & \tan \zeta \cot \beta \end{pmatrix}. \quad (32)$$

The mass of the first pseudoscalar Higgs boson $\phi_1^{0I} \equiv A_1$ is given by

$$M_{A_1}^2 = 2k^2 \lambda_2 - (\alpha_2 - \alpha_3)k(\cot^2 \beta + \cot^2 \zeta) - \frac{1}{\sqrt{2}}k\mu_3 \cot \beta \cot \zeta. \quad (33)$$

The matrix M_I^2 can be diagonalized by the unitary transformation $U^\dagger M_I^2 U = \text{diag}(M_{A_2}^2, 0, 0)$,

$$\begin{pmatrix} \phi_2^{0I} \\ \chi_L^{0I} \\ \chi_R^{0I} \end{pmatrix} = \underbrace{\begin{pmatrix} \frac{1}{\sqrt{\tan^2\beta + \tan^2\zeta + 1}} & -\frac{\tan\zeta}{\sqrt{\tan^2\zeta + 1}} & \frac{\tan\beta}{\sqrt{(\tan^2\zeta + 1)(\tan^2\beta + \tan^2\zeta + 1)}} \\ -\frac{\tan\beta}{\sqrt{\tan^2\beta + \tan^2\zeta + 1}} & 0 & \frac{\sqrt{\tan^2\zeta + 1}}{\sqrt{\tan^2\beta + \tan^2\zeta + 1}} \\ \frac{\tan\zeta}{\sqrt{\tan^2\beta + \tan^2\zeta + 1}} & \frac{1}{\sqrt{\tan^2\zeta + 1}} & \frac{\tan\beta \tan\zeta}{\sqrt{(\tan^2\zeta + 1)(\tan^2\beta + \tan^2\zeta + 1)}} \end{pmatrix}}_U \begin{pmatrix} A_2 \\ G_1^0 \\ G_2^0 \end{pmatrix}, \quad (34)$$

where G_1^0 and G_2^0 are the neutral Goldstone bosons eaten by the gauge bosons Z and Z' to acquire their masses. The other CP -odd Higgs bosons mass is given by

$$M_{A_2}^2 = -\frac{k\mu_3}{\sqrt{2}} \frac{1 + \tan^2\beta + \tan^2\zeta}{\tan\beta \tan\zeta}. \quad (35)$$

It is worth mentioning that $M_{A_2}^2$ constrains the parameter μ_3 to be negative. We find that the typical values of CP -odd Higgs masses are of $\mathcal{O}(100)$ GeV.

(3) CP -even Higgs bosons

Finally, we consider the CP -even Higgs bosons. Similar to the CP -odd Higgs, the squared mass matrix of CP -even Higgs bosons is given by

$$M_{R_{ij}}^2 = \left. \frac{\partial^2 V(\Phi, \chi_{L,R})}{\partial \phi_i^{0R} \partial \phi_j^{0R}} \right|_{\langle \phi_{i,j}^{0R} \rangle = \langle \phi_{i,j}^{0I} \rangle = 0}. \quad (36)$$

Again, one finds that $H_1 = \phi_1^{0R}$ is decoupled with mass $M_{H_1} = M_{A_1}$. The remaining squared mass matrix of the CP -even Higgs bosons is given in the basis $(\phi_2^{0R}, \chi_L^{0R}, \chi_R^{0R})$ by

$$M_R^2 = \begin{pmatrix} k^2\lambda_1 - \frac{k\mu_3}{2\sqrt{2}} \cot\beta \cot\zeta & \alpha_{12}k^2 \cot\beta + \frac{k\mu_3}{2\sqrt{2}} \cot\zeta & \alpha_{12}k^2 \cot\zeta + \frac{k\mu_3}{2\sqrt{2}} \cot\beta \\ \alpha_{12}k^2 \cot\beta + \frac{k\mu_3}{2\sqrt{2}} \cot\zeta & k^2\lambda_3 \cot^2\beta - \frac{k\mu_3}{2\sqrt{2}} \tan\beta \cot\zeta & k^2\lambda_3 \cot\beta \cot\zeta - \frac{k\mu_3}{2\sqrt{2}} \\ \alpha_{12}k^2 \cot\zeta + \frac{k\mu_3}{2\sqrt{2}} \cot\beta & k^2\lambda_3 \cot\beta \cot\zeta - \frac{k\mu_3}{2\sqrt{2}} & k^2\lambda_3 \cot^2\zeta - \frac{k\mu_3}{2\sqrt{2}} \tan\zeta \cot\beta \end{pmatrix}. \quad (37)$$

This matrix can be diagonalized by a unitary transformation: $T^\dagger M_R^2 T = \text{diag}(M_{H_2}^2, M_{H_3}^2, M_H^2)$. The lightest eigenstate H is the SM-like Higgs, the mass of which we will fix to be 125 GeV. In general, from the numerical checks, we found that three CP -even Higgs bosons (H and $H_{1,3}$) are light [of $\mathcal{O}(100)$ GeV], and the other one H_2 is heavy [of $\mathcal{O}(1)$ TeV].

C. Couplings of the SM-like Higgs

From the Yukawa Lagrangian (2), one finds that the SM-like Higgs couplings with fermions in the ALRM are given by

$$Y_{H\bar{u}u} = \frac{m_u}{v} \frac{T_\Phi}{\sin\beta}, \quad Y_{H\bar{d}d} = \frac{m_d}{v} \frac{T_L}{\cos\beta}, \quad Y_{H\bar{d}'d'} = \frac{m_{d'}}{v_R} T_R, \quad (38)$$

$$Y_{H\bar{e}e} = \frac{m_e}{v} \frac{T_\Phi}{\sin\beta}, \quad Y_{H\bar{n}n} = \frac{m_n}{v_R} T_R, \quad (39)$$

where the elements T_Φ, T_L , and T_R are the mixing couplings of the gauge eigenstates ϕ_2^{0R}, χ_L^{0R} , and χ_R^{0R} ,

respectively, with the lightest Higgs H . Similarly, from the kinetic Lagrangian of the scalars, one can derive the following SM-like Higgs couplings with the electroweak gauge bosons,

$$g_{HWW} = gM_W(T_\Phi \sin\beta + T_L \cos\beta), \quad (40)$$

$$g_{HW'W'} = gM_W \left(T_\Phi \sin\beta + T_R \frac{v_R}{v} \right), \quad (41)$$

$$g_{HZZ} = g_{LL} \cos^2\vartheta + g_{LR} \sin\vartheta \cos\vartheta + g_{RR} \sin^2\vartheta, \quad (42)$$

$$g_{HZ'Z'} = g_{LL} \sin^2\vartheta - g_{LR} \sin\vartheta \cos\vartheta + g_{RR} \cos^2\vartheta, \quad (43)$$

where

$$g_{LL} = \frac{gM_W}{\cos^2\theta_w} (T_\Phi \sin\beta + T_L \cos\beta), \quad (44)$$

$$g_{LR} = -\frac{\sqrt{2}gM_W}{\cos^2\theta_w \sqrt{\cos 2\theta_w}} (T_\Phi \cos\beta \cos 2\theta_w - T_L \sin\beta \sin^2\theta_w), \quad (45)$$

$$g_{RR} = \frac{gM_W}{\sqrt{2}\cos^2\theta_w \cos 2\theta_w} \left(T_\Phi \cos\beta \cos^2 2\theta_w + T_L \sin\beta \sin^4\theta_w + T_R \frac{v_R}{v} \cos^4\theta_w \right). \quad (46)$$

Finally, the SM-like Higgs couplings with the charged Higgs bosons are given by

$$\lambda_{HH^\pm H_1^\mp} = M_{1\Phi} T_\Phi + M_{1L} T_L + M_{1R} T_R, \quad (47)$$

$$\lambda_{HH^\pm H_2^\mp} = M_{2\Phi} T_\Phi + M_{2L} T_L + M_{2R} T_R, \quad (48)$$

where

$$M_{1\Phi} = 2(k\lambda_1 \cos^2\beta - v_L(\alpha_2 - \alpha_3) \cos\beta \sin\beta + k\alpha_{13} \sin^2\beta), \quad (49)$$

$$M_{1L} = 2(v_L\alpha_{13} \cos^2\beta - k(\alpha_2 - \alpha_3) \cos\beta \sin\beta + v_L\lambda_3 \sin^2\beta), \quad (50)$$

$$M_{1R} = 2v_R\alpha_{12} \cos^2\beta - \sqrt{2}\mu_3 \cos\beta \sin\beta + \sin^2\beta(2v_R\lambda_3 - \sqrt{2}\mu_3 \tan\beta), \quad (51)$$

$$M_{2\Phi} = 2(k\lambda_1 \cos^2\zeta - v_R(\alpha_2 - \alpha_3) \cos\zeta \sin\zeta + k\alpha_{13} \sin^2\zeta), \quad (52)$$

$$M_{2L} = 2v_L\alpha_{12} \cos^2\zeta - \sqrt{2}\mu_3 \cos\zeta \sin\zeta + \sin^2\zeta(2v_L\lambda_3 - \sqrt{2}\mu_3 \tan\zeta), \quad (53)$$

$$M_{2R} = 2(v_R\alpha_{13} \cos^2\zeta - k(\alpha_2 - \alpha_3) \cos\zeta \sin\zeta + v_R\lambda_3 \sin^2\zeta). \quad (54)$$

IV. ALRM EFFECTS IN $H \rightarrow \gamma\gamma$ DECAY

As advocated in the Introduction, CMS and ATLAS collaborations observed a SM-like Higgs boson with mass around 125 GeV and signal decay strengths as given in Eqs. (55)–(60). For instance, CMS found [14–16]

$$\mu_{\gamma\gamma} = \mu(H \rightarrow \gamma\gamma) = 1.14_{-0.23}^{+0.26}, \quad (55)$$

$$\mu_{ZZ} = \mu(H \rightarrow ZZ) = 0.91_{-0.24}^{+0.3}, \quad (56)$$

$$\mu_{WW} = \mu(H \rightarrow WW) = 0.76 \pm 0.21, \quad (57)$$

while the ATLAS experiment reported that the signal strength of these decays are given by [13,17,18]

$$\mu_{\gamma\gamma} = \mu(H \rightarrow \gamma\gamma) = 1.17 \pm 0.27, \quad (58)$$

$$\mu_{ZZ} = \mu(H \rightarrow ZZ) = 1.7 \pm 0.5, \quad (59)$$

$$\mu_{WW} = \mu(H \rightarrow WW) = 1.01 \pm 0.31. \quad (60)$$

These results indicate enhancement in the diphoton decay channel, with more than 2σ deviation, which could be a very important signal for possible new physics beyond the SM. Much work has been done to accommodate these results in different extensions of the SM [26–35]. The Higgs signal strength of the decay channel, $H \rightarrow \gamma\gamma$, relative to the SM expectation is defined as

$$\begin{aligned} \mu_{\gamma\gamma} &= \frac{\sigma(pp \rightarrow H \rightarrow \gamma\gamma)}{\sigma(pp \rightarrow H \rightarrow \gamma\gamma)^{\text{SM}}} \\ &= \frac{\sigma(pp \rightarrow H)}{\sigma(pp \rightarrow H)^{\text{SM}}} \frac{\text{BR}(H \rightarrow \gamma\gamma)}{\text{BR}(H \rightarrow \gamma\gamma)^{\text{SM}}} \\ &= \frac{\Gamma(H \rightarrow gg)}{\Gamma(H \rightarrow gg)^{\text{SM}}} \frac{\Gamma_{\text{tot}}^{\text{SM}}}{\Gamma_{\text{tot}}} \frac{\Gamma(H \rightarrow AA)}{\Gamma(H \rightarrow \gamma\gamma)^{\text{SM}}} \\ &= \kappa_{gg} \cdot \kappa_{\text{tot}}^{-1} \cdot \kappa_{\gamma\gamma}, \end{aligned} \quad (61)$$

where $\sigma(pp \rightarrow H)$ is the total Higgs production cross section and $\text{BR}(H \rightarrow \gamma\gamma)$ is the branching ratio of the corresponding channel. The total Higgs decay width is given by the sum of the dominant Higgs partial decay widths, $\Gamma_{\text{tot}} = \Gamma_{b\bar{b}} + \Gamma_{WW} + \Gamma_{ZZ} + \Gamma_{gg} + \Gamma_{\tau\bar{\tau}}$. Other partial decay widths are much smaller and can be safely neglected. In the SM with 125 GeV Higgs mass, these partial decay widths are given by $\Gamma_{b\bar{b}} = 2.3 \times 10^{-3}$ GeV, $\Gamma_{WW} = 8.7 \times 10^{-4}$ GeV, $\Gamma_{ZZ} = 1.1 \times 10^{-4}$ GeV, $\Gamma_{gg} = 3.5 \times 10^{-4}$, and $\Gamma_{\tau\bar{\tau}} = 2.6 \times 10^{-4}$ GeV. As shown in the previous section, the Higgs couplings g_{HWW} and $Y_{Hb\bar{b}}$ may slightly change from the SM values. Hence, the total decay width of the Higgs boson remains very close to the SM result. This has been confirmed numerically, and to a very good approximation, one can consider $\kappa_{\text{tot}} \simeq 1$.

Now, we turn to the SM-like Higgs decay into a diphoton, W^+W^- and ZZ in our ALRM. As shown in the previous section, the low-energy effective theory of the ALRM contains two charged Higgs bosons that can be light, of $\mathcal{O}(100)$ GeV, and may give relevant contributions to the SM-like Higgs decay into a diphoton. In addition, the couplings of the SM-like Higgs with a top quark and W gauge boson may be suppressed or even flipped, which would lead to significant enhancement/suppression in $\Gamma(H \rightarrow \gamma\gamma)$. The Feynman diagrams of the Higgs decay $H \rightarrow \gamma\gamma$, mediated by the gauge bosons W^\pm , top quark, and light-charged Higgs bosons are shown in Fig. 1. Note that in the conventional LRM there are interaction vertices among charged Higgs, the W boson, and the neutral Higgs/photon; therefore, another four diagrams with W^\pm and H^\pm running in the loop of triangle diagrams can be generated. In our ALRM, these vertices identically vanish due to the

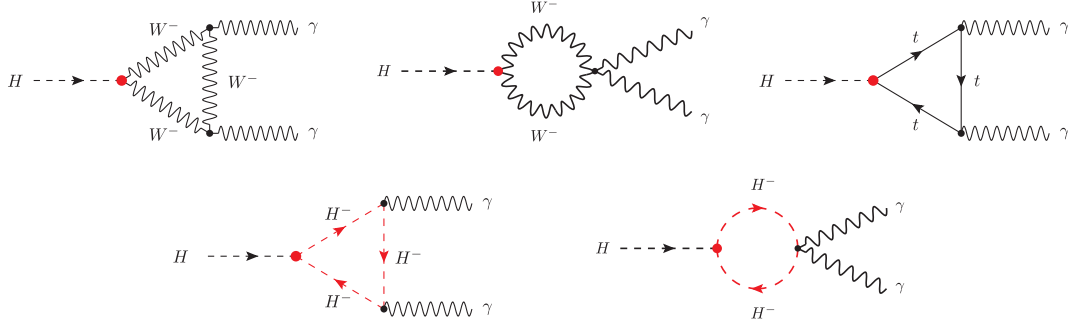


FIG. 1 (color online). Feynman diagrams for the Higgs decay $H \rightarrow \gamma\gamma$ mediated by gauge bosons W^\pm , a top quark, and charged scalars H^\pm .

discrete S symmetry. In this case, the one-loop partial decay width of the H decay into two photons is given by [26]

$$\Gamma(H \rightarrow \gamma\gamma) = \frac{\alpha^2 m_H^3}{1024\pi^3} \left| \frac{g_{HWW}}{M_W^2} Q_W^2 F_1(x_W) + N_{c,t} Q_t^2 \frac{2Y_{H\bar{t}t}}{m_t} F_{1/2}(x_t) + \sum_{i=1}^2 Q_{H_i^\pm}^2 \frac{\lambda_{HH_i^\pm H_i^\mp}}{M_{H_i^\pm}^2} F_0(x_{H_i^\pm}) \right|^2, \quad (62)$$

where $x_t = M_H^2/4m_t^2$, $x_k = M_H^2/4M_k^2$, $k = W, H_{1,2}^\pm$. The color factor and electric charges are given by $N_{c,t} = 3$, $Q_W = Q_{H_i^\pm} = 1$, and $Q_t = 2/3$. Recall that the relevant Higgs couplings in the ALRM are given by g_{HWW} , $Y_{H\bar{t}t}$, and $\lambda_{HH_i^\pm H_i^\mp}$ in Eqs. (39), (40), (47), and (48), with $T_\Phi \sim T_L \gg T_R$. Finally, the loop functions $F_i(x)$ are given by [26]

$$F_1(x) = -[2x^2 + 3x + 3(2x - 1)\arcsin^2(\sqrt{x})]x^{-2}, \quad (63)$$

$$F_{1/2}(x) = 2[x + (x - 1)\arcsin^2(\sqrt{x})]x^{-2}, \quad (64)$$

$$F_0(x) = -[x - \arcsin^2(\sqrt{x})]x^{-2}. \quad (65)$$

For Higgs mass of order 125 GeV and charged Higgs mass of order 200 GeV, the loop functions $F_1(x_W)$, $F_{1/2}(x_t)$, and $F_0(x_{H_i^\pm})$ are of order -8.32 , $+1.38$, and $+0.43$, respectively. Therefore, the partial decay width $\Gamma(H \rightarrow \gamma\gamma)$ can be enhanced through one of the following possibilities: (i) large charged Higgs couplings such that $\lambda_{HH_i^\pm H_i^\mp}/M_{H_i^\pm}^2$ is of order g_{HWW}/M_W^2 and with an opposite sign to compensate the difference in sign between $F_1(x_W)$ and $F_0(x_{H_i^\pm})$; (ii) either the sign of the top Yukawa coupling, $Y_{H\bar{t}t}$, or the sign of the coupling between the W boson and the SM-like Higgs, g_{HWW} , is flipped so that a constructive interference between W -gauge boson and top-quark contributions takes place; and (iii) a significant reduction for the top Yukawa coupling, $Y_{H\bar{t}t}$, to minimize the destructive interference between W and t contributions. In Fig. 2, we display the changes in g_{HWW} and $Y_{H\bar{t}t}$, normalized to their SM values. As can be seen from this figure, both couplings are slightly changed from their expectations in the SM. In addition, both g_{HWW} and $Y_{H\bar{t}t}$ may flip their sign simultaneously, and hence the usual destructive interference between W -gauge boson and top-quark contributions remains intact. Therefore, one would not expect any enhancement of $\Gamma(H \rightarrow \gamma\gamma)$. The sign correlation between the coupling ratios can be understood from the fact that the parameters T_Φ and T_L in Eqs. (39) and

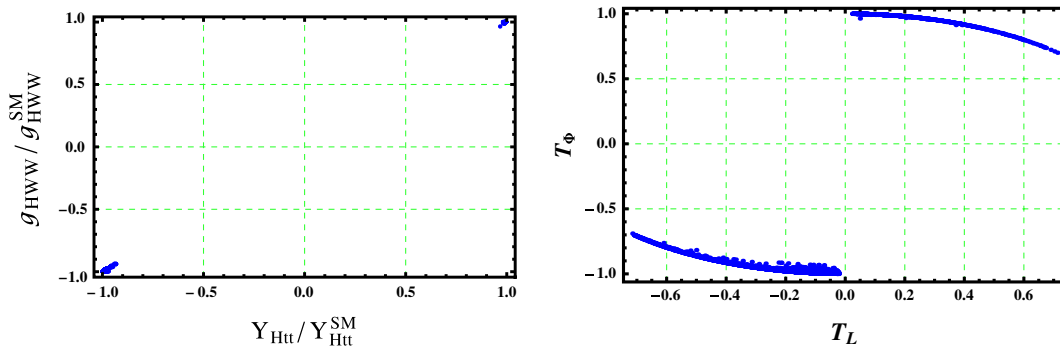


FIG. 2 (color online). (Left panel) The relation between the coupling ratios $g_{HWW}/g_{HWW}^{\text{SM}}$ and $Y_{H\bar{t}t}/Y_{H\bar{t}t}^{\text{SM}}$. (Right panel) The relation between the mixing parameters T_Φ and T_L .

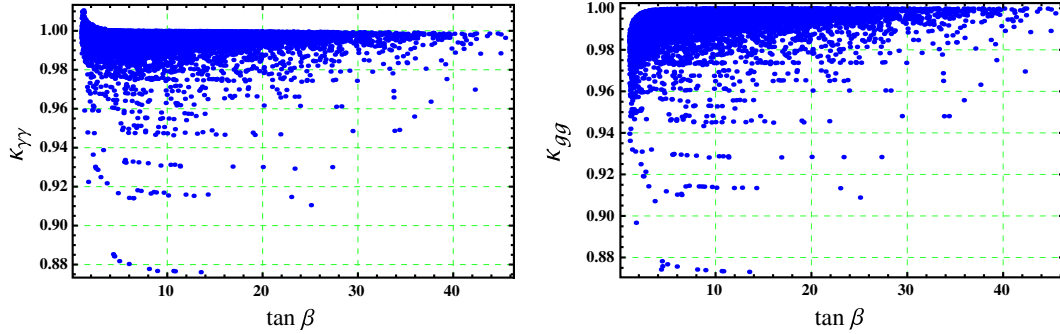


FIG. 3 (color online). $\kappa_{\gamma\gamma}$ and κ_{gg} as functions of $\tan\beta$ and the parameters $\lambda_3, \alpha_1, \alpha_2$, and $M_{H_{1,2}^\pm}$.

(40), which lead to the modifications of these couplings, have the same sign in the allowed region of ALRM parameter space, as shown in Fig. 2.

The Higgs boson production at the LHC is dominated by gluon-gluon fusion. As in the SM, this channel is mediated by top quarks via a one-loop triangle diagram. The extra quark d' gives a negligible contribution to $\sigma(gg \rightarrow H)$ due to the suppression of its coupling with the SM-like Higgs and also its large mass. As mentioned, the top Yukawa coupling can be slightly different from the SM coupling; therefore, the ratio $\kappa_{gg} = \Gamma(H \rightarrow gg)/\Gamma(H \rightarrow gg)^{\text{SM}}$ can be slightly deviated from 1.

In Fig. 3, we display the results of $\kappa_{\gamma\gamma} = \Gamma(H \rightarrow \gamma\gamma)/\Gamma(H \rightarrow \gamma\gamma)^{\text{SM}}$ and κ_{gg} as function of $\tan\beta$ for $0 < \lambda_1, \lambda_3, \lambda_4 < \sqrt{4\pi}$, $-\sqrt{4\pi} < \lambda_2 < 0$, $-\sqrt{4\pi} < \alpha_1$, $\alpha_2, \alpha_3 < \sqrt{4\pi}$, $100 < M_{H_{1,2}^\pm} < 300$, and $\mu_3 < 0$, to be consistent with the perturbative unitarity and the minimization and boundedness from below conditions (21)–(24). It is worth mentioning that for $\mu_3 < 0$ one finds, from the minimization conditions, that $\lambda_4 - \lambda_3 > 0$, and from (21), $\lambda_3 \geq 0$ and hence $\lambda_4 > \lambda_3 \geq 0$. In our numerical analysis, we express the parameters μ_1^2 , μ_2^2 , and λ_4 in terms of the three vevs v_L , v_R , and k (or v , $\tan\beta$, and $M_{W'}$). We also substitute the parameters μ_3 and α_3 in terms of the charged Higgs masses $M_{H_{1,2}^\pm}$ and the parameter λ_1 in terms of the SM-like Higgs mass $M_H = 125$ GeV. Thus, one can write the matrix $T \equiv T(\tan\beta, M_{W'}, M_{H_{1,2}^\pm}, \lambda_3, \alpha_1, \alpha_2)$. This figure

confirms our theoretical expectation and shows that both of $\kappa_{\gamma\gamma}$ and κ_{gg} can slightly deviate from 1.

In this case, it is clear that the signal strength $\mu_{\gamma\gamma}$ is also close to the SM expectation and can be still consistent with both ATLAS and CMS experimental results. In Fig. 4, we show the signal strength as a function of $\tan\beta$, where other parameters are scanned in the above-mentioned regions. For completeness, we also present the correlation between $\mu_{\gamma\gamma}$ and μ_{ZZ} , which equals μ_{WW} in our model. It is remarkable that all signal strengths of Higgs decay channels in the ALRM are slightly less than the SM results.

V. SIGNATURES AT THE LHC

In this section, we study the interesting signatures of the exotic quark d' associated with our ALRM at the LHC. In particular, we will analyze and compute the cross section for the production of this heavy quark and its subsequent decays into jets, leptons, and missing energy. The Lagrangian of d' interactions with the SM quarks can be derived from (2) as

$$\mathcal{L}_Y^{d'} = -\bar{u}(\cos\zeta Y^q P_R + \sin\zeta Y_R^q P_L)H_2^+ V'_{\text{CKM}} d' + \text{H.c.}, \quad (66)$$

where V'_{CKM} is the right-handed quark mixing matrix. In addition, the kinetic Lagrangian of d' leads to the interactions with the gauge bosons

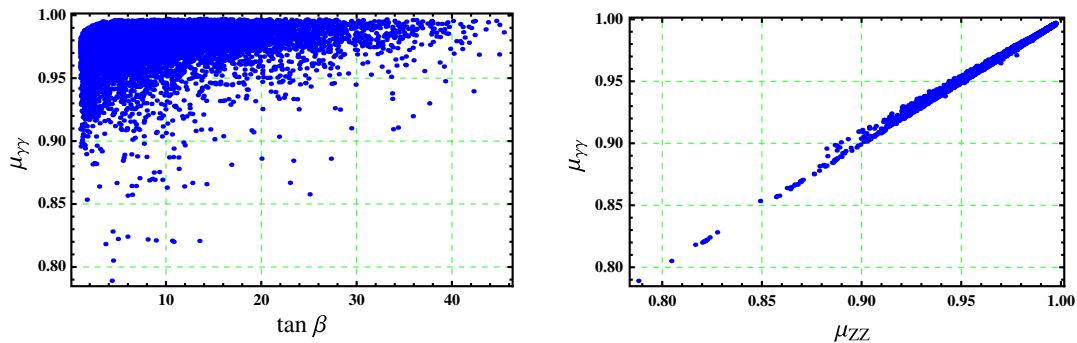


FIG. 4 (color online). (Left panel) The signal strength $\mu_{\gamma\gamma}$ as a function of $\tan\beta$ and the parameters $\lambda_3, \alpha_1, \alpha_2$, and $M_{H_{1,2}^\pm}$. (Right panel) Correlation between $\mu_{\gamma\gamma}$ and μ_{ZZ} in the ALRM.

$$\begin{aligned}
\mathcal{L}_{\text{gauge}}^{d'} = & -\frac{ig_s}{2} \bar{d}' \gamma^\mu \lambda_a G_\mu^a d' - \frac{ig}{\sqrt{2}} \bar{u} P_R \gamma^\mu W_\mu^{'+} V'_{\text{CKM}} d' \\
& - \frac{ig}{\sqrt{2}} \bar{d}' \gamma^\mu P_R W_\mu^{'-} V'_{\text{CKM}} u \\
& + \frac{i}{3} e \bar{d}' \gamma^\mu \left[A_\mu + \left(\hat{P} \sin \vartheta - \frac{1}{2} \tan \theta_w \cos \vartheta \right) Z_\mu \right. \\
& \left. + \left(\hat{P} \cos \vartheta + \frac{1}{2} \tan \theta_w \sin \vartheta \right) Z'_\mu \right] d', \quad (67)
\end{aligned}$$

where

$$\hat{P} = \frac{3 \cos 2\theta_w - \sin^2 \theta_w}{6 \sin \theta_w \cos \theta_w \sqrt{\cos 2\theta_w}} P_R + \frac{\sin \theta_w}{\cos \theta_w \sqrt{\cos 2\theta_w}} P_L, \quad (68)$$

where λ_a 's, $a = 1, \dots, 8$, are the Gell–Mann matrices and ϑ is given in (15). Accordingly, in this case, the pair production of d' at the LHC is dominated by the following channel: $gg \rightarrow d' \bar{d}'$. Considering all contributions from s, t, and u channels, the squared amplitude of this process is given by

$$\begin{aligned}
|\mathcal{M}(gg \rightarrow d' \bar{d}')|^2 = & \frac{g_s^4}{24 \hat{s}^2} \frac{(9m_{d'}^4 - 9m_{d'}^2(\hat{s} + 2\hat{t}) + 4\hat{s}^2 + 9\hat{s}\hat{t} + 9\hat{t}^2)}{(m_{d'}^2 - \hat{t})^2} \\
& \times \left[\frac{m_{d'}^2(\hat{s}^3 + 2\hat{s}^2\hat{t} + 8\hat{s}\hat{t}^2 + 8\hat{t}^3) + \hat{t}(\hat{s} + \hat{t})(\hat{s}^2 + 2\hat{s}\hat{t} + 2\hat{t}^2)}{(-m_{d'}^2 + \hat{s} + \hat{t})^2} \right. \\
& \left. - \frac{2m_{d'}^8 - 8m_{d'}^6\hat{t} + m_{d'}^4(3\hat{s}^2 + 4\hat{s}\hat{t} + 12\hat{t}^2)}{(-m_{d'}^2 + \hat{s} + \hat{t})^2} \right]. \quad (69)
\end{aligned}$$

In addition, the squared amplitude of the pair production of d' through the channel $q\bar{q} \rightarrow \gamma/g \rightarrow d' \bar{d}'$ is given by

$$\begin{aligned}
|\mathcal{M}(q\bar{q} \rightarrow \gamma/g \rightarrow d' \bar{d}')|^2 = & \frac{4(2g^4 + 9g_s^4)}{81 \hat{s}^2} (2\hat{s}\hat{t} - 4(m_q^2 + m_{d'}^2)\hat{t}) \\
& + 2(m_q^2 + m_{d'}^2)^2 + 2\hat{t}^2 + \hat{s}^2, \quad (70)
\end{aligned}$$

where \hat{s}, \hat{t} are the partonic Mandelstam variables. The differential cross section is given by

$$\frac{d\hat{\sigma}}{d \cos \theta} = \frac{B}{16\pi \hat{s}^2} |\mathcal{M}|^2, \quad (71)$$

where $B = \sqrt{1 - (4m_{d'}^2/\hat{s})}$. The cross section of $pp \rightarrow d' \bar{d}'$ is given by

$$\frac{d\sigma}{d \cos \theta} = \sum_{i,j} \int_{x_0}^1 dx f_i(x) f_j \left(\frac{4m_{d'}^2}{sx} \right) \frac{d\hat{\sigma}}{d \cos \theta}, \quad (72)$$

where i, j refer to the partons. The partons energy fractions are given by $x_1 x_2 = \hat{s}/s$, so that the minimum parton energy fraction to produce the $d' \bar{d}'$ pair is $x_0 = 2m_{d'}/\sqrt{s}$. Also, $\hat{t} = -\frac{1}{2}\hat{s}(1 - B \cos \theta) + M_{d'}^2$. Therefore, one finds that the production cross section is given by

$$\frac{d\hat{\sigma}}{d\hat{t}} = \frac{1}{8\pi \hat{s}^3} |\mathcal{M}|^2. \quad (73)$$

In Fig. 5, we display the differential cross section of the $d' \bar{d}'$ pair production at the LHC with $\sqrt{s} = 14$ TeV as a function of the invariant mass $M_{d' \bar{d}'}$ for two choices of $m_{d'}$, namely, $m_{d'} = 300$ and 500 GeV. As can be seen from this figure, the typical value of the d' production cross section is of $\mathcal{O}(1)$ fb, which was quite accessible at the LHC during its second run. The dominant decay channel of the produced d' quark is given by $d' \rightarrow H_2^+ u$, as indicated in (66). One can show that the corresponding decay rate is given by

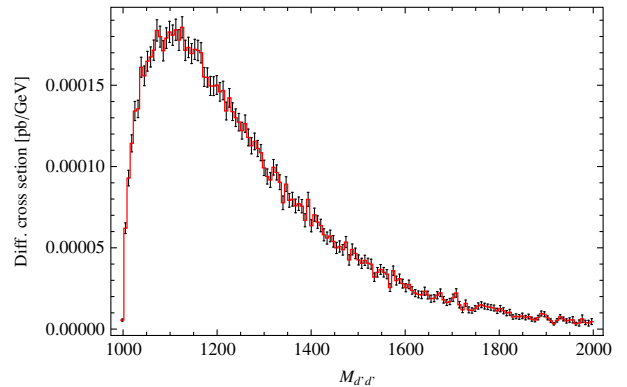
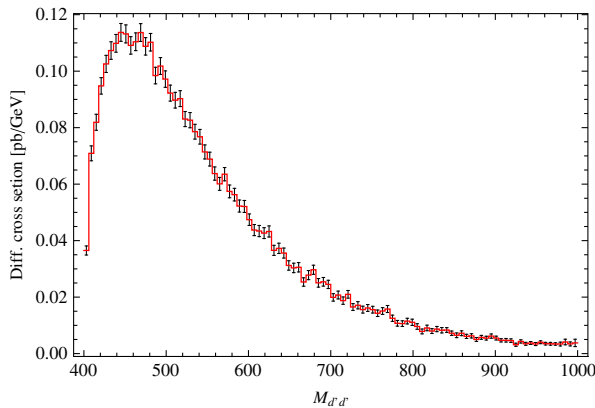
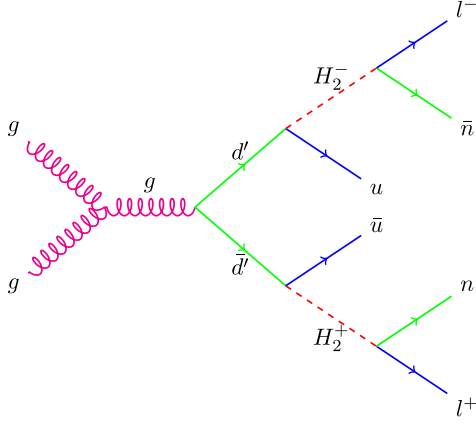
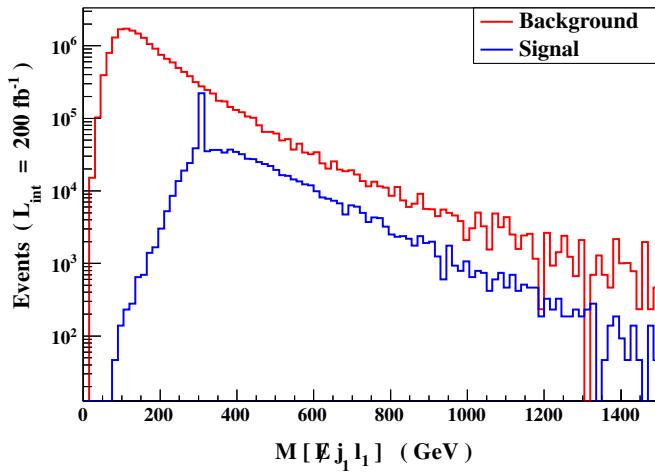
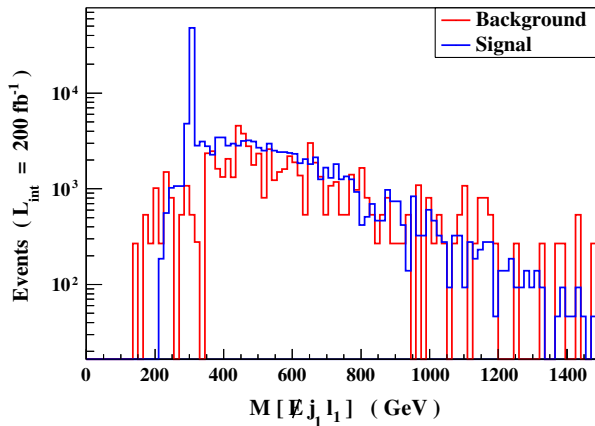


FIG. 5 (color online). Differential production cross section of exotic quark d' as a function of the invariant mass $M_{d' \bar{d}'}$. In the left panel, $m_{d'} = 300$ GeV, and in the right panel, $m_{d'} = 500$ GeV.


 FIG. 6 (color online). The exotic quark, d' , creation and decay.

 FIG. 7 (color online). The reconstructed invariant mass of the extra quark, d' , which decays to $l + \text{jet} + \text{missing energy}$ and its background for $m_{d'} = 300$ GeV. No cut has been imposed yet.


$$\Gamma(d' \rightarrow uH_2^+) = \frac{|V'_{\text{CKM}}|^2}{16\pi\hbar} (|Y^q|^2 \cos^2\zeta + |Y_R^q|^2 \sin^2\zeta) \times m_{d'} \left(1 - \frac{M_{H_2^+}^2}{m_{d'}^2}\right)^2. \quad (74)$$

Here, we assumed that $m_u \ll m_{d'}$. On the other hand, the charged Higgs boson H_2^+ decays into a lepton and scotino through the interactions

$$\mathcal{L}_Y^{H_2^+} = \bar{n}H_2^+U'_{\text{MNS}}(\cos\zeta Y^\ell P_L + \sin\zeta Y_R^\ell P_R)e + \text{H.c.} \quad (75)$$

Thus, the decay rate of $H_2^- \rightarrow e^-n$, for $m_e = 0$, is given by

$$\Gamma(H_2^- \rightarrow e^-n) = \frac{|U'_{\text{MNS}}|^2}{16\pi\hbar} (|Y^\ell|^2 \cos^2\zeta + |Y_R^\ell|^2 \sin^2\zeta) \times M_{H_2^+} \left(1 - \frac{m_n^2}{M_{H_2^+}^2}\right)^2. \quad (76)$$

In Fig. 6, we show the total cross section of this process with an opposite-sign dilepton, which is the most striking signature for this exotic quark at the LHC. This cross section can be approximately written as

$$\begin{aligned} \sigma(gg \rightarrow g \rightarrow d'\bar{d}' \rightarrow l^\mp l^\pm + E_T^{\text{miss}} + \text{jets}) \\ \simeq \sigma(gg \rightarrow g \rightarrow d'\bar{d}') \\ \times \text{BR}(d' \rightarrow H_2^+ + \text{jets})^2 \text{BR}(H_2^\mp \rightarrow l^\mp + E_T^{\text{miss}})^2. \quad (77) \end{aligned}$$

Since the dominant decay channel of d' is $d' \rightarrow uH_2^-$ and the charged Higgs decays mainly to $l^\pm + n$, one finds $\text{BR}(d' \rightarrow uH_2^-) \simeq 1$ and $\text{BR}(H_2^\pm \rightarrow l^\pm n) \simeq 1$. Therefore, $\sigma(gg \rightarrow g \rightarrow d'\bar{d}' \rightarrow l^\mp l^\pm + E_T^{\text{miss}} + \text{jets}) \simeq \sigma(gg \rightarrow g \rightarrow d'\bar{d}') \simeq \mathcal{O}(1)$ fb, which can be accessible at the LHC with

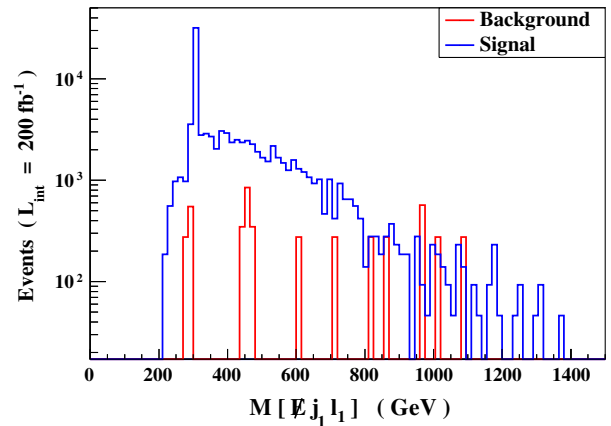

 FIG. 8 (color online). The reconstructed invariant mass of the extra quark, d' , which decays to $l + \text{jet} + \text{missing energy}$ for $m_{d'} = 300$ GeV, with the $E_T > 200$ GeV cut (left panel) and $H_T < 200$ GeV cut (right panel).

TABLE II. Signal vs background for the process $pp \rightarrow d'd' \rightarrow (l^-l^+) + (u\bar{u}) + (nn)$ with/without cuts.

Cuts (GeV)	Signal (S)	Background (B)	S vs B
Initial (no cut)	463999	9309732 ± 21646	0.049840 ± 0.000116
Cut 1 ($E_T > 200$)	72291 ± 247	33523 ± 198	2.1564 ± 0.0148
Cut 2 ($H_T < 200$)	47977 ± 207	1942.7 ± 44.3	24.696 ± 0.573

$\sqrt{s} \approx 14$ TeV. In Fig. 7, we show the reconstructed invariant mass of the extra quark d' , which decays into $l + n(\text{scotino}) + \text{jet}$, with all possible background. In this figure, we have not imposed any cut yet. Therefore, the background is clearly dominates the signal. Here, we assume $m_{d'} = 300$ GeV, the charged Higgs mass is of order 200 GeV, and the LHC integrated luminosity is of order 200 fb^{-1} .

In Fig. 8 (left panel), we plot the number of reconstructed events per bin of the invariant mass of d' of the above process for signal and SM background at $E_T \text{ cut} > 200$ GeV, where E_T is the missing transverse energy, $E_T = \|\sum_{\text{visible particles}} \vec{p}_T\|$, with $m_{d'} = 300$ GeV and $\sqrt{s} = 14$ TeV. This figure shows that it is possible to extract a good significance for the extra-quark signal in this channel. In addition, we also impose a cut, $H_T < 200$ GeV, where H_T is the total transverse hadronic energy: $H_T = \sum_{\text{hadronic particles}} \|\vec{p}_T\|$. It is remarkable that with H_T cuts the signal can be much larger than the background. We have used Feynrules [36] to generate the model files and Calchep [37] and MadEvent5 [38,39] to calculate the numerical values of the cross sections and number of events, respectively.

Finally, we provide in Table II some details for the used cuts on P_T and H_T on the signal and background for the process $pp \rightarrow d'd' \rightarrow (l^-l^+) + (u\bar{u}) + (nn)$. As can be seen from the results in this table, the signal of this process can be much larger than the background if one imposes the proper H_T cuts. It is worth mentioning that the Higgs sector of our model is very similar to the two Higgs doublets in the minimal supersymmetric standard model, where one Higgs doublet couples to up quarks and the second couples to down quarks. Therefore, it does not lead to any flavor-changing neutral current problem, and a light charged Higgs is phenomenologically acceptable. The number of events of exotic quark d' at the LHC may be slightly changed if a heavier charged Higgs is considered, but with keeping $m_{H^\pm} < m_{d'}$, to ensure that $\text{BR}(d \rightarrow H^\pm + \text{jets}) \sim 1$.

VI. CONCLUSIONS

In this paper, we have analyzed some phenomenological aspects of the alternative left-right model, motivated by the superstring-inspired E_6 model. We provided a detailed analysis for the symmetry breaking and Higgs sector of this model, which consists of four neutral CP -even Higgs,

two CP -odd Higgs, and two charged Higgs bosons. We emphasized that three neutral CP -even Higgs and two CP -odd Higgs in addition to two charged Higgs can be light, of $\mathcal{O}(100)$ GeV. We also found that the contributions of charged Higgs bosons and the extra exotic quark d' to $H \rightarrow \gamma\gamma$ are quite negligible. Therefore, our model predicts signal strengths of Higgs decay, in particular, of $H \rightarrow \gamma\gamma$ and $H \rightarrow W^+W^-$ that coincide with the SM expectations.

Finally, we studied the striking signatures of the exotic down-type quark at the LHC. In particular, we computed the cross section of d' -pair production. We showed that the typical value of this cross section is of $\mathcal{O}(1)$ fb, which is quite accessible at the LHC. The decay of d' into a jet, lepton, and missing energy provides an important signature for this class of models at the LHC.

ACKNOWLEDGMENTS

This work is partially supported by the Abdus Salam International Centre for Theoretical Physics (ICTP) Grant No. AC-80. M. Ashry would like to thank W. Abdallah, A. Elsayed, A. Hammad, and A. Moursy for fruitful discussions.

APPENDIX

To study the boundedness from below, and hence the stability, of the potential (20), we use the following theorem [24,25] to ensure that the matrix of the quartic terms, which are dominant at higher values of the fields, is copositive:

Theorem 1 (copositivity criteria): Let $a \in \mathbb{R}, b \in \mathbb{R}^{n-1}$ and $C \in \mathbb{R}^{(n-1) \times (n-1)}$. The symmetric matrix $M \in \mathbb{R}^{n \times n}$,

$$M = \begin{pmatrix} a & b^T \\ b & C \end{pmatrix},$$

is copositive if and only if:

- (1) $a \geq 0, C$ is copositive,
- (2) for any nonzero vector $y \in \mathbb{R}^{(n-1)}$, with $y \geq 0$, if $b^T y \leq 0$, it follows that $y^T (aC - bb^T) y \geq 0$.

The quartic terms of the potential (20) can be written as

$$\begin{aligned}
{}^{4F}V(\phi_{1,2}^{0,+}, \chi_{L,R}^{0,+}) &= \lambda_1(|\phi_1^0|^4 + |\phi_1^+|^4 + |\phi_2^0|^4 + |\phi_2^+|^4) + \lambda_3(|\chi_L^0|^4 + |\chi_L^+|^4 + |\chi_R^0|^4 + |\chi_R^+|^4) \\
&+ 2|\phi_1^0|^2[\lambda_1(|\phi_1^+|^2 + |\phi_2^+|^2) + \lambda_{12}|\phi_2^0|^2 + \alpha_{13}(|\chi_L^0|^2 + |\chi_R^0|^2) + \alpha_{12}(|\chi_L^+|^2 + |\chi_R^+|^2)] \\
&+ 2|\phi_1^+|^2[\lambda_1|\phi_2^0|^2 + \lambda_{12}|\phi_2^+|^2 + \alpha_{13}(|\chi_L^0|^2 + |\chi_R^0|^2) + \alpha_{12}(|\chi_L^+|^2 + |\chi_R^+|^2)] \\
&+ 2|\phi_2^0|^2[\lambda_1|\phi_2^+|^2 + \alpha_{12}(|\chi_L^0|^2 + |\chi_R^0|^2) + \alpha_{13}(|\chi_L^+|^2 + |\chi_R^+|^2)] \\
&+ 2|\phi_2^+|^2[\alpha_{12}(|\chi_L^0|^2 + |\chi_R^0|^2) + \alpha_{13}(|\chi_L^+|^2 + |\chi_R^+|^2)] \\
&+ 2|\chi_L^0|^2(\lambda_3|\chi_L^+|^2 + \lambda_4|\chi_R^0|^2 + \lambda_4|\chi_R^+|^2) + 2|\chi_L^+|^2(\lambda_4|\chi_R^0|^2 + \lambda_4|\chi_R^+|^2) \\
&+ 2\lambda_3|\chi_R^0|^2|\chi_R^+|^2 - 8\lambda_2\text{Re}[\phi_1^0\phi_1^-\phi_2^0\phi_2^+] \\
&+ 4(\alpha_2 - \alpha_3)\text{Re}[(\phi_1^0\phi_2^+ + \phi_2^{0*}\phi_1^+)\chi_L^0\chi_L^- + (\phi_2^0\phi_2^+ + \phi_1^{0*}\phi_1^+)\chi_R^0\chi_R^-], \tag{A1}
\end{aligned}$$

where $\alpha_{12} = \alpha_1 + \alpha_2$, $\alpha_{13} = \alpha_1 + \alpha_3$, and $\lambda_{12} = \lambda_1 + 2\lambda_2$. We have

$$\phi_{1,2}^{0,+} = |\phi_{1,2}^{0,+}| \exp[i\theta_{1,2}^{0,+}], \quad \chi_{L,R}^{0,+} = |\chi_{L,R}^{0,+}| \exp[i\theta_{L,R}^{0,+}]. \tag{A2}$$

By the redefinitions of the fields' components,

$$\begin{aligned}
\phi_1^+ &\rightarrow \phi_1^+ \exp[i(\theta_1^0 - \theta_1^+)], & \phi_2^0 &\rightarrow \phi_2^0 \exp[i(\theta_1^0 - \theta_2^0)], \\
\phi_2^+ &\rightarrow \phi_2^+ \exp[-i(\theta_1^0 + \theta_2^+)], \tag{A3}
\end{aligned}$$

$$\chi_{L,R}^+ \rightarrow \chi_{L,R}^+ \exp[i(\theta_{L,R}^0 - \theta_{L,R}^+)], \tag{A4}$$

we can write

$$\begin{aligned}
{}^{4F}V(\phi_{1,2}^{0,+}, \chi_{L,R}^{0,+}) &= X^T {}^{4F}V X - 8\lambda_2|\phi_1^0||\phi_1^-||\phi_2^0||\phi_2^+| \\
&+ 4(\alpha_2 - \alpha_3)[(|\phi_1^0||\phi_2^+| + |\phi_2^0||\phi_1^+|)|\chi_L^0||\chi_L^+| \\
&+ (|\phi_2^0||\phi_2^+| + |\phi_1^0||\phi_1^+|)|\chi_R^0||\chi_R^+|], \tag{A5}
\end{aligned}$$

where

$$X^T = (|\phi_1^0|^2 \quad |\phi_1^+|^2 \quad |\phi_2^0|^2 \quad |\phi_2^+|^2 \quad |\chi_L^0|^2 \quad |\chi_L^+|^2 \quad |\chi_R^0|^2 \quad |\chi_R^+|^2), \tag{A6}$$

$${}^{4F}V = \begin{pmatrix} \lambda_1 & \lambda_1 & \lambda_{12} & \lambda_1 & \alpha_{13} & \alpha_{12} & \alpha_{13} & \alpha_{12} \\ \lambda_1 & \lambda_1 & \lambda_1 & \lambda_{12} & \alpha_{13} & \alpha_{12} & \alpha_{12} & \alpha_{13} \\ \lambda_{12} & \lambda_1 & \lambda_1 & \lambda_1 & \alpha_{12} & \alpha_{13} & \alpha_{12} & \alpha_{13} \\ \lambda_1 & \lambda_{12} & \lambda_1 & \lambda_1 & \alpha_{12} & \alpha_{13} & \alpha_{13} & \alpha_{12} \\ \alpha_{13} & \alpha_{13} & \alpha_{12} & \alpha_{12} & \lambda_3 & \lambda_3 & \lambda_4 & \lambda_4 \\ \alpha_{12} & \alpha_{12} & \alpha_{13} & \alpha_{13} & \lambda_3 & \lambda_3 & \lambda_4 & \lambda_4 \\ \alpha_{13} & \alpha_{12} & \alpha_{12} & \alpha_{13} & \lambda_4 & \lambda_4 & \lambda_3 & \lambda_3 \\ \alpha_{12} & \alpha_{13} & \alpha_{13} & \alpha_{12} & \lambda_4 & \lambda_4 & \lambda_3 & \lambda_3 \end{pmatrix}. \tag{A7}$$

For the potential (A1) to be bounded from below, it must happen that the matrix ${}^{4F}V$ is copositive and $\lambda_2 \leq 0$ and

$\alpha_2 - \alpha_3 \geq 0$. The pseudoscalar Higgs mass (35) implies that $\mu_3 < 0$. With the minimization condition (22), both imply that $\lambda_4 > \lambda_3$. The copositivity implies that the diagonal elements $\lambda_1, \lambda_3 \geq 0$. Accordingly, $\lambda_4 > \lambda_3 \geq 0$. It is remarkable that the copositivity of the matrix ${}^{4F}V$ significantly depends on the signs of the parameters α_{12}, α_{13} , and λ_{12} . Here, we present the cases depending on these signs:

- (1) $\alpha_{12} \geq 0, \alpha_{13} \geq 0$, and $\lambda_{12} \geq 0$: In this case, the matrix ${}^{4F}V$ is copositive, and the potential is bounded from below.
- (2) $\alpha_{12} \geq 0, \alpha_{13} \geq 0$, and $\lambda_{12} \leq 0$: The copositivity conditions are

$$\lambda_1 + \lambda_2 \geq 0, \quad \lambda_1^2 + 8\lambda_1\lambda_2 + 4\lambda_2^2 \leq 0. \tag{A8}$$

We deduce these conditions in detail considering the case assumptions and using Theorem 1. To make the 8×8 matrix ${}^{4F}V$ be copositive, we shall make that first with the 7×7 matrix, C , arising from the matrix ${}^{4F}V$ by eliminating the first row and the first column. In our case, it is sufficient to stop at this level, since the 6×6 matrix, C_1 , arising from the matrix ${}^{4F}V$ by eliminating the first two rows and the first two columns is already copositive, being a matrix of nonnegative elements. Now,

$${}^{4F}V = \begin{pmatrix} \lambda_1 & b^T \\ b & C \end{pmatrix}, \quad b^T = (\lambda_1 \quad \lambda_{12} \quad \lambda_1 \quad \alpha_{13} \quad \alpha_{12} \quad \alpha_{13} \quad \alpha_{12}), \tag{A9}$$

$$C = \begin{pmatrix} \lambda_1 & b_1^T \\ b_1 & C_1 \end{pmatrix}, \quad b_1^T = (\lambda_1 \quad \lambda_{12} \quad \alpha_{13} \quad \alpha_{12} \quad \alpha_{12} \quad \alpha_{13}). \tag{A10}$$

Let $y_1^T = (x_1 x_2 x_3 x_4 x_5 x_6)$ be a vector that satisfies Theorem 1 requests, i.e., a nonzero and a non-negative vector. Taking $x_2 \neq 0, x_{1,3,\dots,6} = 0$, makes

the linear form $b_1^T y_1 = \lambda_{12} x_2 \leq 0$ and its corresponding quadratic form

$$y_1^T (\lambda_1 C_1 - b_1 b_1^T) y_1 = -4\lambda_2 (\lambda_1 + \lambda_2) x_2^2.$$

Since we have $\lambda_2 \leq 0$, we impose the condition

$$\lambda_1 + \lambda_2 \geq 0 \quad (\text{A11})$$

to make the quadratic form $y_1^T (\lambda_1 C_1 - b_1 b_1^T) y_1 \geq 0$ and hence as a necessary condition for the copositivity.

Let us assume that $x_i \neq 0, i = 1, \dots, 6$. Then, the linear form

$$b_1^T y_1 \leq 0 \iff x_2 \geq x_2^{\min} = \frac{1}{-\lambda_{12}} (\lambda_1 x_1 + \alpha_{13} x_3 + \alpha_{12} x_4 + \alpha_{12} x_5 + \alpha_{13} x_6).$$

The copositivity condition (A11) makes the corresponding quadratic form be increasing in x_2 (for any fixed values of the other x_i 's), and hence we deduce that

$$\begin{aligned} y_1^T (\lambda_1 C_1 - b_1 b_1^T) y_1 \geq y_1^T (\lambda_1 C_1 - b_1 b_1^T) y_1 |_{x_2=x_2^{\min}} &= \frac{\lambda_1}{\lambda_{12}^2} [4\lambda_1 \lambda_2^2 x_1^2 - 2\lambda_2 (\alpha_{13} \lambda_1 - \alpha_{12} \lambda_{12}) x_1 x_3 - 2\lambda_2 (\alpha_{12} \lambda_1 - \alpha_{13} \lambda_{12}) x_1 x_4 \\ &+ 2x_1 ((\alpha_{12} x_5 + \alpha_{13} x_6) (\lambda_1^2 + 2\lambda_1 \lambda_2 + 4\lambda_2^2) - 2(\alpha_{13} x_5 + \alpha_{12} x_6) \lambda_1 \lambda_{12}) \\ &+ x_3 ((\alpha_{13}^2 \lambda_1 - 2\alpha_{12} \alpha_{13} \lambda_{12}) (x_3 + 2x_6) + \lambda_{12}^2 (\lambda_3 x_3 + 2\lambda_4 x_6)) \\ &+ 2x_3 ((\alpha_{12} \alpha_{13} \lambda_1 - \lambda_{12} (\alpha_{12}^2 + \alpha_{13}^2)) (x_4 + x_5) + \lambda_{12}^2 (\lambda_3 x_4 + \lambda_4 x_5)) \\ &+ x_4 ((\alpha_{12}^2 \lambda_1 - 2\alpha_{12} \alpha_{13} \lambda_{12}) (x_4 + 2x_5) + \lambda_{12}^2 (\lambda_3 x_4 + 2\lambda_4 x_5)) \\ &+ 2x_6 ((\alpha_{12} \alpha_{13} \lambda_1 - \lambda_{12} (\alpha_{12}^2 + \alpha_{13}^2)) (x_4 + x_5) + \lambda_{12}^2 (\lambda_4 x_4 + \lambda_3 x_5)) \\ &+ (\alpha_{12}^2 \lambda_1 - 2\alpha_{12} \alpha_{13} \lambda_{12} + \lambda_{12}^2 \lambda_3) x_5^2 + (\alpha_{13}^2 \lambda_1 - 2\alpha_{12} \alpha_{13} \lambda_{12} + \lambda_{12}^2 \lambda_3) x_6^2]. \end{aligned} \quad (\text{A12})$$

By the case assumptions and the copositivity condition (A11), the quadratic form (A12) is non-negative termwise, and the theorem is satisfied.

For the copositivity of the matrix 4FV , let $y^T = (x_1 x_2 x_3 x_4 x_5 x_6 x_7)$ be a nonzero and a non-negative vector. Let $x_{1,2,3} \neq 0, x_{4,\dots,7} = 0$. Then, the linear form

$$b^T y = \lambda_1 (x_1 + x_3) + \lambda_{12} x_2 \leq 0$$

$$\iff x_2 \geq x_2^{\min} = \frac{\lambda_1}{-\lambda_{12}} (x_1 + x_3).$$

Condition (A11) makes the corresponding quadratic form

$$\begin{aligned} y^T (\lambda_1 C - b b^T) y \\ = -4\lambda_2 (x_1 (x_2 - x_3) \lambda_1 + x_2 (x_3 \lambda_1 + x_2 (\lambda_1 + \lambda_2))) \end{aligned}$$

be increasing in x_2 (for any fixed values of $x_{1,3}$), and hence we deduce that

$$\begin{aligned} y^T (\lambda_1 C - b b^T) y \geq y^T (\lambda_1 C - b b^T) y |_{x_2=x_2^{\min}} \\ = \frac{4\lambda_1}{\lambda_{12}^2} (\lambda_1 \lambda_2^2 x_1^2 + \lambda_2 (\lambda_1^2 + 6\lambda_1 \lambda_2 + 4\lambda_2^2) x_1 x_3 + \lambda_1 \lambda_2^2 x_3^2) \geq 0 \\ = \frac{4\lambda_1}{\lambda_{12}^2} X_{13}^T M_{13} X_{13}, \quad \forall x_{1,3}, \end{aligned}$$

where

$$M_{13} = \begin{pmatrix} \lambda_1 \lambda_2^2 & \frac{1}{2} \lambda_2 (\lambda_1^2 + 6\lambda_1 \lambda_2 + 4\lambda_2^2) \\ \frac{1}{2} \lambda_2 (\lambda_1^2 + 6\lambda_1 \lambda_2 + 4\lambda_2^2) & \lambda_1 \lambda_2^2 \end{pmatrix}, \quad X_{13} \begin{pmatrix} x_1 \\ x_3 \end{pmatrix}.$$

Now, $y^T(\lambda_1 C - bb^T)y|_{x_2=x_2^{\min}} \geq 0$ is equivalent to the copositivity of the matrix M_{13} . Equivalently,

$$\lambda_1^2 + 8\lambda_1\lambda_2 + 4\lambda_2^2 \leq 0. \quad (\text{A13})$$

Now, assume that $x_i \neq 0, i = 1, \dots, 7$. Then, the linear form

$$\begin{aligned} b^T y \leq 0 &\iff x_2 \geq x_2^{\min} \\ &= \frac{1}{-\lambda_{12}}(\lambda_1 x_1 + \lambda_1 x_3 + \alpha_{13} x_4 + \alpha_{12} x_5 \\ &\quad + \alpha_{13} x_6 + \alpha_{12} x_7). \end{aligned}$$

As before, conditions (A11), (A13) make

$$\begin{aligned} y^T(\lambda_1 C - bb^T)y &\geq y^T(\lambda_1 C - bb^T)y|_{x_2=x_2^{\min}} \geq 0, \\ &\forall x_{1,3,\dots,6}. \end{aligned}$$

Hence, the theorem is satisfied, and, finally, the only imposed conditions for the matrix ${}^{4F}V$ to be copositive in this case are those in (A8). The same procedure is followed to extract the copositivity conditions in the following cases:

- (3) $\alpha_{12} \geq 0, \alpha_{13} \leq 0$, and $\lambda_{12} \geq 0$: The following conditions are necessary for the copositivity:

$$\lambda_1\lambda_3 - \alpha_{13}^2 \geq 0, \quad \alpha_{13}^2(\lambda_3 - \lambda_4) \geq 0.$$

Since $\lambda_4 - \lambda_3 > 0$, then we must have $\alpha_{13} = 0$. Finally, in this case, the copositivity conditions are

$$\alpha_{12} \geq 0, \quad \alpha_{13} = 0, \quad \lambda_{12} \geq 0. \quad (\text{A14})$$

- (4) $\alpha_{12} \leq 0, \alpha_{13} \geq 0$, and $\lambda_{12} \geq 0$: The following conditions are necessary for the copositivity:

$$\lambda_1\lambda_3 - \alpha_{12}^2 \geq 0, \quad \alpha_{12}^2(\alpha_{12} - \alpha_{13})^2\lambda_1^2(\lambda_3^2 - \lambda_4^2) \geq 0.$$

Again, either $\alpha_{12} = 0, \alpha_{12} = \alpha_{13}$, or $\lambda_1 = 0$. But the minimal copositivity conditions in this case are

$$\alpha_{12} = 0, \quad \alpha_{13} \geq 0, \quad \lambda_{12} \geq 0. \quad (\text{A15})$$

- (5) $\alpha_{12} \geq 0, \alpha_{13} \leq 0$, and $\lambda_{12} \leq 0$: The copositivity conditions are

$$\begin{aligned} \alpha_{12} \geq 0, \quad \alpha_{13} = 0, \quad \lambda_{12} \leq 0, \\ \lambda_1 + \lambda_2 \geq 0, \quad \lambda_1^2 + 8\lambda_1\lambda_2 + 4\lambda_2^2 \leq 0. \end{aligned} \quad (\text{A16})$$

- (6) $\alpha_{12} \leq 0, \alpha_{13} \geq 0$, and $\lambda_{12} \leq 0$: The copositivity conditions are

$$\begin{aligned} \alpha_{12} = 0, \quad \alpha_{13} \geq 0, \quad \lambda_{12} \leq 0, \\ \lambda_1 + \lambda_2 \geq 0, \quad \lambda_1^2 + 8\lambda_1\lambda_2 + 4\lambda_2^2 \leq 0. \end{aligned} \quad (\text{A17})$$

- (7) $\alpha_{12} \leq 0, \alpha_{13} \leq 0$, and $\lambda_{12} \geq 0$: The following conditions are necessary for the copositivity:

$$\begin{aligned} \lambda_1\lambda_3 - \alpha_{12}^2 \geq 0, \quad \lambda_1\lambda_3 - \alpha_{13}^2 \geq 0, \\ \alpha_{12}^2(\lambda_3 - \lambda_4) \geq 0, \quad \alpha_{13}^2(\lambda_3 - \lambda_4) \geq 0. \end{aligned} \quad (\text{A18})$$

Hence, in this case, the copositivity conditions are

$$\alpha_{12} = \alpha_{13} = 0, \quad \lambda_{12} \geq 0. \quad (\text{A19})$$

- (8) $\alpha_{12} \leq 0, \alpha_{13} \leq 0$, and $\lambda_{12} \leq 0$: The copositivity conditions are

$$\begin{aligned} \alpha_{12} = \alpha_{13} = 0, \quad \lambda_{12} \leq 0, \\ \lambda_1 + \lambda_2 \geq 0, \quad \lambda_1^2 + 8\lambda_1\lambda_2 + 4\lambda_2^2 \leq 0. \end{aligned} \quad (\text{A20})$$

-
- [1] R. Mohapatra and J. C. Pati, *Phys. Rev. D* **11**, 2558 (1975).
[2] G. Senjanovic and R. N. Mohapatra, *Phys. Rev. D* **12**, 1502 (1975).
[3] R. N. Mohapatra, F. E. Paige, and D. Sidhu, *Phys. Rev. D* **17**, 2462 (1978).
[4] N. Deshpande, J. Gunion, B. Kayser, and F. I. Olness, *Phys. Rev. D* **44**, 837 (1991).
[5] C. S. Aulakh, A. Melfo, and G. Senjanovic, *Phys. Rev. D* **57**, 4174 (1998).
[6] A. Maiezza, M. Nemevsek, F. Nesti, and G. Senjanovic, *Phys. Rev. D* **82**, 055022 (2010).
[7] D. Borah, S. Patra, and U. Sarkar, *Phys. Rev. D* **83**, 035007 (2011).
[8] M. Nemevsek, G. Senjanovic, and V. Tello, *Phys. Rev. Lett.* **110**, 151802 (2013).
[9] E. Ma, *Phys. Rev. D* **36**, 274 (1987).
[10] K. Babu, X.-G. He, and E. Ma, *Phys. Rev. D* **36**, 878 (1987).
[11] E. Ma, *J. Phys. Conf. Ser.* **315**, 012006 (2011).
[12] S. Khalil, H.-S. Lee, and E. Ma, *Phys. Rev. D* **81**, 051702 (2010).
[13] K. Cheung, J. S. Lee, and P.-Y. Tseng, *Phys. Rev. D* **90**, 095009 (2014).
[14] V. Khachatryan *et al.* (CMS Collaboration), *Eur. Phys. J. C* **74**, 3076 (2014).
[15] C. Ochoando (CMS Collaboration), Rencontres de Moriond, QCD Session, LHC, CERN, 2013 (unpublished),

- <http://moriond.in2p3.fr/QCD/2013/ThursdayMorning/Ochando.pdf>.
- [16] CMS PAS HIG-13-005, <http://cds.cern.ch/record/1542387/files/HIG-13-005-pas.pdf>.
- [17] E. Mountricha (ATLAS Collaboration), Rencontres de Moriond, QCD Session, Brookhaven National Laboratory, 2013 (unpublished), <http://moriond.in2p3.fr/QCD/2013/ThursdayMorning/Mountricha2.pdf>.
- [18] ATLAS-CONF-2013-034, <http://cds.cern.ch/record/1528170/files/ATLAS-CONF-2013-034.pdf>.
- [19] E. Ma, *Phys. Rev. D* **85**, 091701 (2012).
- [20] S. Chatrchyan *et al.* (CMS Collaboration), *J. High Energy Phys.* **08** (2012) 023.
- [21] G. Aad *et al.* (ATLAS Collaboration), *Phys. Lett. B* **705**, 28 (2011).
- [22] G. Aad *et al.* (ATLAS Collaboration), *Phys. Rev. Lett.* **107**, 272002 (2011).
- [23] S. Chatrchyan *et al.* (CMS Collaboration), *J. High Energy Phys.* **05** (2011) 093.
- [24] L. Ping and F. Y. Yu, *Linear Algebra Appl.* **194**, 109 (1993).
- [25] K. Kannike, *Eur. Phys. J. C* **72**, 2093 (2012).
- [26] M. Carena, I. Low, and C. E. Wagner, *J. High Energy Phys.* **08** (2012) 060.
- [27] W. Chao, J.-H. Zhang, and Y. Zhang, *J. High Energy Phys.* **06** (2013) 039.
- [28] I. Picek and B. Radovicic, *Phys. Lett. B* **719**, 404 (2013).
- [29] W.-F. Chang, J. N. Ng, and J. M. Wu, *Phys. Rev. D* **86**, 033003 (2012).
- [30] P. S. B. Dev, D. K. Ghosh, N. Okada, and I. Saha, *J. High Energy Phys.* **03** (2013) 150; **05** (2013) 049.
- [31] T. Basak and S. Mohanty, *J. High Energy Phys.* **08** (2013) 020.
- [32] J. Cao, P. Wan, J. M. Yang, and J. Zhu, *J. High Energy Phys.* **08** (2013) 009.
- [33] W.-Z. Feng and P. Nath, *Phys. Rev. D* **87**, 075018 (2013).
- [34] M. Berg, I. Buchberger, D. Ghilencea, and C. Petersson, *Phys. Rev. D* **88**, 025017 (2013).
- [35] S. Khalil and S. Salem, *Nucl. Phys.* **B876**, 473 (2013).
- [36] A. Alloul, N. D. Christensen, C. Degrande, C. Duhr, and B. Fuks, *Comput. Phys. Commun.* **185**, 2250 (2014).
- [37] A. Belyaev, N. D. Christensen, and A. Pukhov, *Comput. Phys. Commun.* **184**, 1729 (2013).
- [38] J. Alwall, M. Herquet, F. Maltoni, O. Mattelaer, and T. Stelzer, *J. High Energy Phys.* **06** (2011) 128.
- [39] E. Conte, B. Fuks, and G. Serret, *Comput. Phys. Commun.* **184**, 222 (2013).